

NUCLEAR RESONANCE STUDIES WITH RELATIVISTIC AND RADIOACTIVE BEAMS*

H. EMLING

Gesellschaft für Schwerionenforschung (GSI),
D-64291 Darmstadt, Germany

(Received December 9, 1997)

Secondary beams of radioactive ions at high energies are used at GSI to explore the nuclear structure of exotic nuclei. This report concentrates on the investigation of halo nuclei located at the neutron dripline. Relevant reaction mechanisms such as nuclear and electromagnetic break-up are discussed together with the nuclear structure information that can be deduced.

PACS numbers: 25.60. -t, 24.70. Ef, 27.20. +n

1. Introduction

Secondary ion beams of unstable nuclei at high or intermediate energies have developed into a currently very active field of nuclear structure research far off stability. Such beams are available at a number of laboratories spread all over the world and new projects are under discussion. At GSI, a secondary heavy ion beam facility is implemented by means of the synchrotron SIS and the Fragment Separator FRS, eventually linked to the storage ring ESR. The SIS provides beams of all elements from hydrogen to uranium with energies in the domain of 1 GeV/nucleon. After extraction from SIS, the primary beam may be directed onto a thick ‘production’ target and be converted into secondary, eventually unstable ion beams. Commonly, the process of nuclear fragmentation, but also fission (in case of a ^{238}U primary beam) are exploited for production of secondary beams. Despite of the high secondary beam energy of typically several hundreds of MeV/nucleon, the strong bending power of the FRS allows for in-flight mono-isotopic separation with very small contaminants. Some applications (see below), however benefit from a ‘mixed’ secondary beam composed of

* Presented at the XXV Mazurian Lakes School of Physics, Piaski, Poland, August 27–September 6, 1997.

isotopes of similar neutron-to-proton ratio and thus likewise of interest, *e.g.* for spectroscopic investigations. Secondary beams can be used at the focal planes of the FRS itself, be injected into the storage ring ESR, or be transported to secondary target stations hosting a variety of experimental setups. The experimental apparatus employed in studies discussed in more detail in Section 2, is shown schematically in Fig. 1. It consists of a combination of the Crystal-Ball γ -spectrometer, the ALADIN magnet, and the neutron detector LAND, in conjunction with a rich variety of heavy-ion or charged particle detectors. Charged and neutral particles and heavy fragments are observed with high detection efficiency and almost complete solid angle coverage, and their momenta are determined after interactions of the unstable beams with the target. Thus a measurement, kinematically complete in the projectile rapidity domain is achieved. The following Section is focussing on secondary beam reactions with neutron-halo nuclei. We discuss the specific reaction mechanisms relevant at high bombarding energies and the nuclear structure information that can be deduced. In Section 3 we give a short summary and outlook.

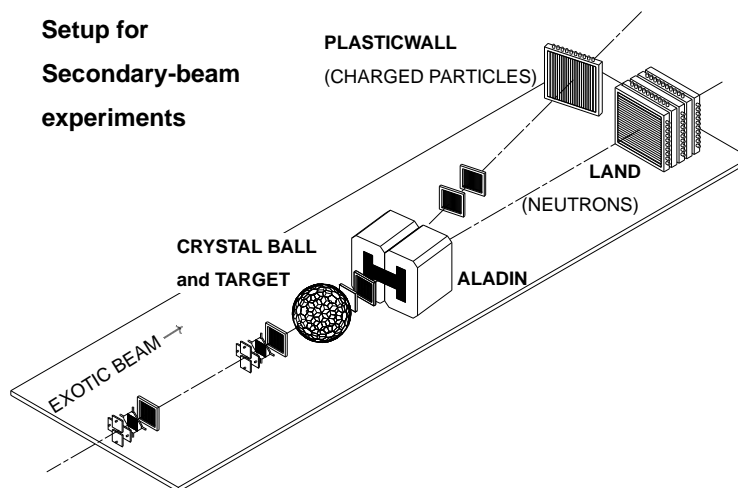


Fig. 1. Schematic view of the experimental setup used for a number of radioactive beam experiments at GSI, partly discussed in Section 2.

2. Neutron-halo nuclei

First evidence for extended neutron matter distributions in some light neutron-rich nuclei at the dripline were derived, in fact, from high-energy fragmentation studies with secondary beams [1]. Initially, ^{11}Li with its two loosely bound valence neutrons, forming a halo around a ^9Li core, found special interest. Meanwhile, numerous studies with secondary beams of halo

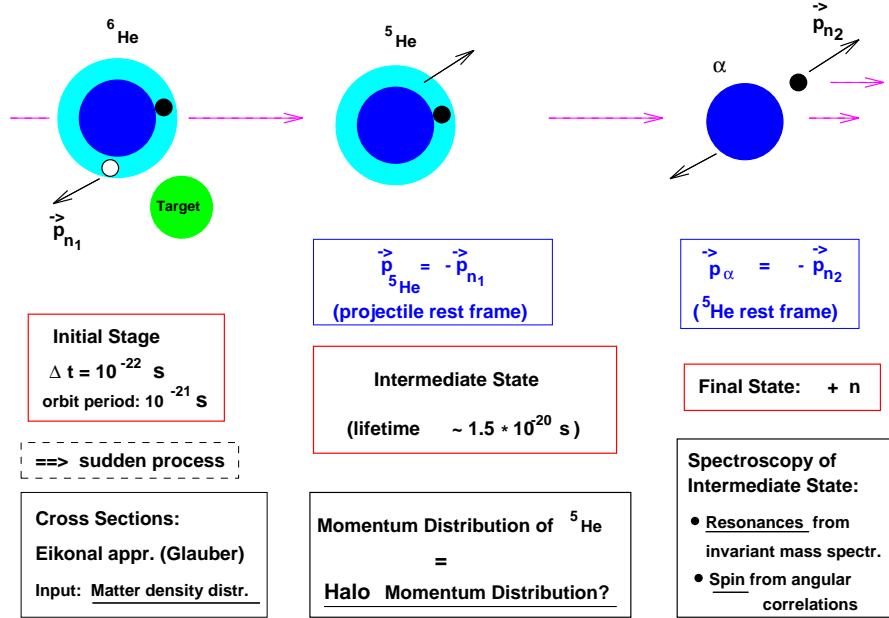


Fig. 2. Schematic illustration of the single-halo-nucleon knock-out reaction, exemplified for a ${}^6\text{He}$ beam. The spectroscopic information that can be deduced from this process is indicated.

nuclei of masses below 20 amu have been performed at various laboratories, aiming at detailed investigations of halo matter and momentum distributions, the underlying single particle structure, clusterisation effects, new collective ('soft') modes *etc.* (for a review see Refs. [2], [3]). At GSI, we studied fragmentation of the halo nuclei ${}^{11}\text{Li}$, ${}^{11,14}\text{Be}$, and ${}^{6,8}\text{He}$ at energies around 200–300 MeV/nucleon on C and Pb targets. Mixed secondary beams composed of such nuclei are extracted by the FRS after bombarding a 4 mg/cm^2 Be target with a primary ${}^{18}\text{O}$ beam (340 MeV/nucleon) and are transferred to the experimental area. The detector setup is very similar to the one shown in Fig. 1, the Crystal-Ball, however, is not implemented. Both, the incident beam ions and the heavy fragments emerging from the target are identified uniquely with regard to nuclear charge and mass, and their momenta were measured; momenta of coincident neutrons are determined as well using the LAND detector. Technical details and results can be found in Refs. [4–8].

Here, we shall focus on 'halo break-up' reactions of the type ${}^6\text{He} \rightarrow {}^6\text{He} + xn$ or ${}^{11}\text{Li} \rightarrow {}^9\text{Li} + xn$, *i.e.* we ensure that the core of the halo nucleus remains intact. Commonly, two basic interaction mechanisms are considered:

— nuclear or electromagnetic inelastic excitation into the continuum or to higher lying resonances. For heavy targets, the electromagnetic excitation dominates. In fact, for ^{11}Li a halo break-up cross section of 2.0(5) barn is observed with the lead target, while the corresponding value with the carbon target amounts to 280(30) mb only;

— knock-out (sometimes referred to as ‘stripping’) of halo neutrons due to collisions with target nucleons. It appears (see below) that the knock-out of a single halo neutron is the predominant process with light targets such as carbon.

We first discuss the knock-out mechanism with emphasis on the nuclear structure information that may be obtained from this process. An illustration, exemplifying the case of ^6He is provided in Fig. 2.

2.1. Knock-out cross sections

In Fig. 3 we show cross sections for halo break-up reactions of ^6He and ^{11}Li on a carbon target in function of the neutron multiplicity registered in LAND. Halo neutrons which are knocked out are scattered to large angles and likely escape from detection in LAND. If a single halo neutron is knocked out, a particle unstable subsystem (*e.g.* ^5He or ^{10}Li) remains — in case of two-neutron halo nuclei — which subsequently undergoes decay into the core nucleus and the ‘spectator’ neutron. The latter one is focussed into a narrow forward angle cone and is detected. Obviously, this process of single nucleon knock-out is predominant as seen from Fig. 3; cross sections associated to an apparent neutron multiplicity of zero or one can be identified (after small corrections) with that of double or single halo-neutron knock-out, respectively. The cross section at neutron multiplicity two can be understood as resulting from inelastic excitation (‘diffractive scattering’) processes being discussed below. The measured cross sections may be compared to Glauber type calculations (eikonal approximation) which require the density distribution both of core and halo nucleons as input. Such calculations were performed for ^6He and ^{11}Li beams on C targets by G. Bertsch *et al.* [9] and are shown in Fig. 3. The density distribution of ^6He is well under control and experimental and calculated cross section agree rather well. For ^{11}Li the situation is less clear: at one hand, the normal shell model level sequence suggests that the two halo neutrons occupy the $1p^{3/2}$ level, at the other hand, however, the valence neutron of the neighboring halo nucleus ^{11}Be occupies the $2s^{1/2}$ intruder orbit. Thus, a considerable mixing of s- and p-states may be expected for ^{11}Li (and as well for the halo nucleus ^{14}Be). In Fig. 3, cross sections calculated for two extreme cases, an uncorrelated s-state and an uncorrelated p-state model, are shown together with a model involving a mixing of s- and p-states (23 % s-state, denoted as

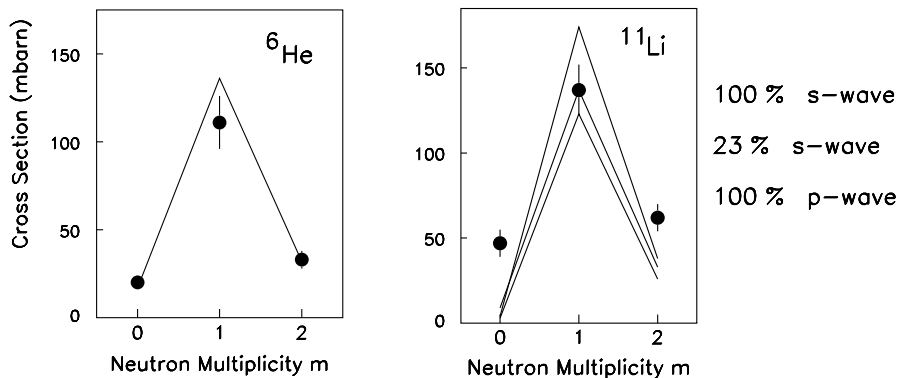


Fig. 3. Left panel: Halo-neutron removal cross sections for ${}^6\text{He}$ at 240 MeV/nucleon as function of the apparent neutron multiplicity measured in LAND. Multiplicities $m = 0, 1, 2$ may be associated to double and single knock-out and inelastic excitation, respectively. The solid curve represents a calculation (eikonal approximation) of Ref. [9] using a well established density profile for ${}^6\text{He}$. Right panel: same as in left panel but for ${}^{11}\text{Li}$. The curves represent calculations [9] using different models for ${}^{11}\text{Li}$ (see text).

‘s23’ in Ref. [9]). None of the calculation is satisfying but a strong mixing of s- and p-states seems indicated. It is one of the main aims of various experiments to identify the single particle structure of halo nuclei such as ${}^{11}\text{Li}$ or ${}^{14}\text{Be}$.

2.2. Momentum distributions

Knock-out of halo nucleons is a fast process during which the internal nucleon degrees of freedom may be considered to be frozen. In this ‘sudden approximation’ the momentum distribution of the residual system (*e.g.* ${}^5\text{He}$, see Fig. 2 for illustration) should thus reflect the internal momentum distribution of the knocked-out halo neutron, if viewed in the projectile rest frame. This picture is very much in the spirit of the Goldhaber model [10] which has been applied successfully in describing momentum distributions of stable nuclei produced in heavy ion fragmentation reactions. The internal momentum distribution of halo nucleons is closely related to their spatial distribution (via Fourier transformation of the respective relative wavefunction). Early attempts intended to derive the halo momentum distribution from measurements of the momentum distributions of the residues, *i.e.* from the core or spectator neutron momentum distributions. Distortions, however, may be caused by several effects: ‘Core shadowing’ could lead to a truncation of the inner part of the halo wavefunction and thus of the high

momentum tails. Final state interaction (FSI), *e.g.* between core and spectator neutron, can spoil the momentum distribution as well. The latter effect, however can be eliminated experimentally, if the momentum distribution of the combined system, core plus spectator neutron, is reconstructed, as it is possible in complete-kinematics experiments considered here. In Fig. 4 we summarize such results from GSI experiments. Evidently, for halo nuclei the momentum distributions are much more narrow than those found for stable nuclei as expected because of the large spatial extension of the halo wavefunction. Secondly, the momentum width seems to depend on the specific single particle structure, *e.g.* the width of the halo neutron in ^{11}Be occupying an s-state is clearly more narrow than that of halo neutrons in He-isotopes occupying p-states. A more detailed analysis of momentum distributions in ^{11}Li [5] revealed an admixture of about 50 % s-state neutrons in ^{11}Li , and the systematics shown in Fig. 4 is indicative of a similar admixture in the case of ^{14}Be .

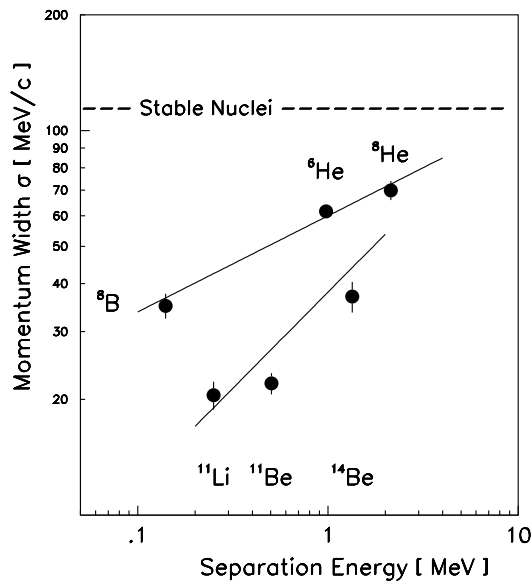


Fig. 4. Systematics of the momentum width σ for halo nucleons as function of neutron (proton) separation energies. For two-neutron halo nuclei, the momentum width is that of one component of the transverse momentum distribution reconstructed from the core and spectator neutron momenta (see text). Data are shown for the two-neutron halo nuclei ^6He [11], ^8He [6], ^{11}Li [20], ^{14}Be [20], the one-neutron halo ^{11}Be [19], and the one-proton halo ^8B [19]. The dashed line indicates a corresponding average value for stable fragments (one nucleon removal).

2.3. Spectroscopy of intermediate particle-unstable resonances

After knock-out of a halo neutron, the final state interaction between the residual core and spectator neutron may give rise to formation of resonances in this subsystem and thus may allow for a spectroscopy of such particle-unbound systems (see Fig. 2 for illustration). The resonances can be visualized utilizing invariant mass spectroscopy, *i.e.* determining the distribution in cross section as function of the relative energy of the two constituents (in their rest frame). Indeed, it was observed that practically the entire cross section observed after single neutron knock-out from ${}^6\text{He}$ and ${}^8\text{He}$ can be attributed to the formation of the known ${}^5\text{He}$ [11] and ${}^7\text{He}$ [7] ground state resonances, respectively. In Fig. 5, we show the corresponding spectrum for ${}^{10}\text{Li}$. Two components are recognized, a fast rising component

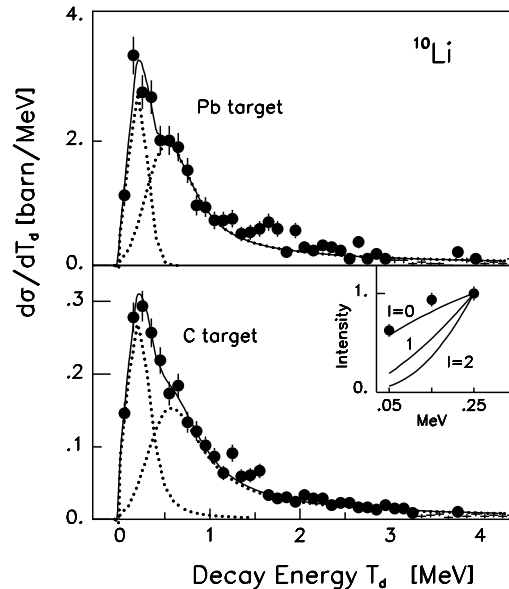


Fig. 5. Decay energy spectra for ${}^{10}\text{Li}$ obtained from an invariant-mass analysis of ${}^9\text{Li}+n$ after break-up of ${}^{11}\text{Li}$ on a C and a Pb target [7]. The spectra are decomposed (dashed lines) as discussed in the text. The inset shows the spectrum at lowest decay energies in comparison to the threshold behaviour of cross sections expected for $l=0, 1, 2$ neutron waves.

right at threshold and a second structure around 500 keV. The first one we assign to the s-wave component, the second one to the p-wave component. This assignment is consistent with recent results from pion absorption data [12] and earlier measurements (see Ref. [7] for more details and further references). A detailed analysis of the spectrum obtained with the carbon

target was performed in [9] and it was concluded that the ^{11}Li halo neutrons are in an s-state with about 30–40 % probability. Our recent measurement for ^{13}Be reveals a very similar result.

An analysis of the angular correlation of the decay of such resonances gives a more direct approach to determine their spin quantum numbers. The momentum of the knocked-out halo neutron, represented by the combined momentum of core and spectator neutron as discussed above, defines a quantization axis. In Fig. 6 we show the angular distribution of the relative core-spectator neutron momentum with respect to this axis. A strong anisotropy is observed, a close inspection [8], shows that the anisotropy, however, is attenuated by about a factor two with respect to that expected for a $0^+ (^6\text{He})\text{--}3/2^-\text{--}(^5\text{He})\text{--}0^+ (^4\text{He})$ correlation. A detailed analysis performed in [13] explains this discrepancy by a small admixture of about 6–7 % resulting from an $0^+ \text{--}1/2^-\text{--}0^+$ correlation, *i.e.* an excitation of the first excited state of ^5He . It thus appears that angular correlation techniques allow for spin assignments of intermediate resonances. At present, angular correlations of that type are analyzed for the ^{10}Li and ^{13}Be resonances.

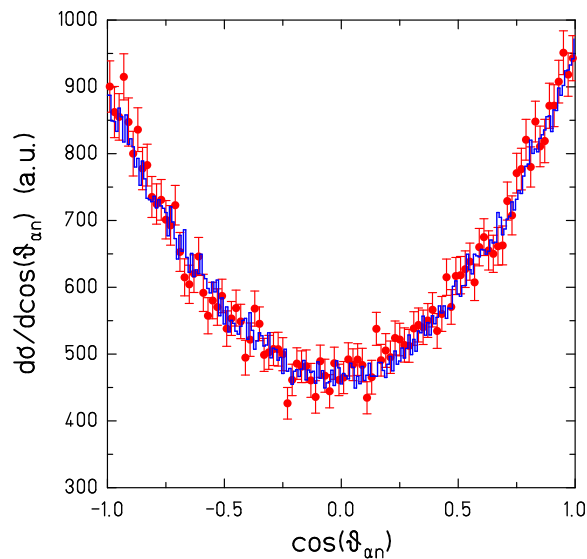


Fig. 6. Angular distribution of the relative ^4He — neutron momentum with respect to the ^5He recoil axis after single neutron knock-out from a ^6He beam on a carbon target [8]. The solid line represents the angular correlation of the $0^+ \text{--} 3/2^- \text{--} 0^+$ sequence attenuated, however, by a factor of two (see text). Instrumental effects are taken into account.

2.4. Inelastic excitations

From Fig. 2 we observe that a small fraction of the halo break-up cross section obtained with the C target yields two neutrons emitted in forward direction. We understand this process as due to inelastic excitations of small momentum and energy transfer. Inelastic excitations can proceed via direct break-up into the continuum or via resonances embedded into the continuum. Calculations of the nuclear inelastic response performed for ${}^6\text{He}$ in the framework of a three-body cluster model [14] indicate that the nuclear response is mainly composed out of quadrupole and dipole excitations. The known 2^+ resonance [15] and a second 2^+ state (not observed so far) carry a large fraction of the quadrupole strength, while the dipole strength is peaked around 2 MeV. Experimentally, the excitation energy spectrum can be obtained from an invariant mass reconstruction involving the core fragment and the two observed neutrons. The GSI data for ${}^6\text{He}$ obtained with the carbon target, show indeed clearly the excitation of the first 2^+ resonance, the second 2^+ state cannot be recognized.

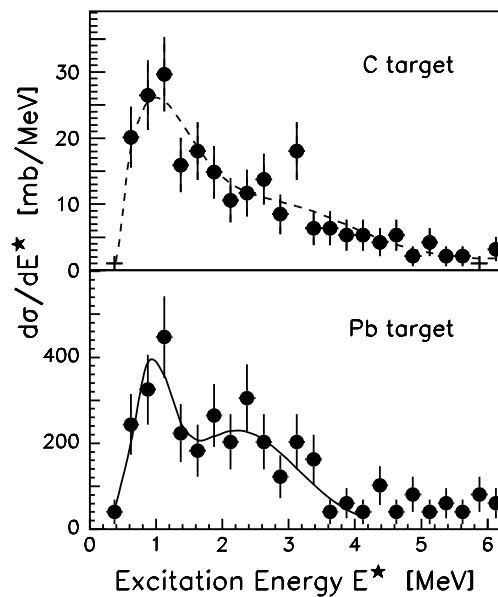


Fig. 7. Excitation energy spectra of inelastic excitation of ${}^{11}\text{Li}$ on a C target (upper panel) and a Pb target (lower panel) [7].

Using a heavy target such as lead, the inelastic excitation is predominantly of electromagnetic nature and is expected to reflect the electric dipole response. The corresponding experimental spectrum for ${}^6\text{He}$ [16] is peaked at around 2.5 MeV excitation energy and to most part, can be reproduced

using the electric dipole response obtained in a three-body cluster model [17] without invoking di-neutron correlations. In contrast, the dipole response obtained within a di-neutron cluster model [18] fails to reproduce the measured cross section. Similar findings are deduced from the ^{11}Li spectrum shown in Fig. 7. Tentatively, the spectrum for the Pb target is decomposed into two components, the first one again can be reproduced by the uncorrelated three-body model, the second one involves more complex excitations (for details see Ref. [7]).

3. Outlook

Secondary beams of exotic nuclei offer new possibilities for nuclear structure research. Specific reaction mechanisms at intermediate or high beam energies are suitable for spectroscopic applications. Here, we only discussed knock-out processes and inelastic excitations, but elastic scattering or charge-changing reactions may be considered as well as a source of nuclear structure information. At present, the interest focuses on light nuclei near the driplines, where new phenomena such as nuclear halos have been discovered. Further developments of the radioactive beam facilities, and drastically improved secondary beam intensities in particular, shall allow to extend such studies towards heavier mass regions. At GSI, an intensity upgrading program is on the way, expected to be effective in 1999, and discussions on long-term projects involving high-intensity beams were already started.

The author is strongly indebted to his colleagues of the LAND and FRS groups and of the S034/S135 collaboration.

REFERENCES

- [1] I. Tanihata *et al.*, *Phys. Rev. Lett.* **55**, 2676 (1985).
- [2] P.G. Hansen, A.S. Jensen, B. Jonson, *Annu. Rev. Nucl. Part. Sci.* **45**, 591 (1995).
- [3] I. Tanihata, *Prog. Part. Nucl. Phys.* **35**, 505 (1995).
- [4] T. Nilsson *et al.*, *Europhys. Lett.* **30**, 19 (1995).
- [5] M. Zinser *et al.*, *Phys. Rev. Lett.* **75**, 1719 (1995).
- [6] T. Nilsson *et al.*, *Nucl. Phys.* **A598**, 418 (1996).
- [7] M. Zinser *et al.*, *Nucl. Phys.* **A619**, 151 (1996).
- [8] L.V. Chulkov *et al.*, *Phys. Rev. Lett.* **79**, 201 (1997).
- [9] G.F. Bertsch, K. Hencken, H. Esbensen, preprint (1997).
- [10] A.S. Goldhaber, *Phys. Lett.* **53B**, 306 (1997).

- [11] D. Aleksandrov *et al.*, GSI-Preprint 97-61 (1997).
- [12] M.G. Gornov *et al.*, Proc. Int. Conf. Nucl. Structure and Related Topics, Dubna (1997).
- [13] L.V. Chulkov, G. Schrieder, preprint TU Darmstadt (1997).
- [14] B.V. Danilin *et al.*, preprint (1997).
- [15] F. Ajzenberg-Selove, *Nucl. Phys.* **A490**, 1 (1988).
- [16] T. Aumann *et al.*, to be published.
- [17] A. Pushkin, B. Jonson, M.V. Zhukov, *J. Phys.* **G22**, L95 (1996).
- [18] C.A. Bertulani, G. Baur, *Phys. Rep.* **163**, 299 (1988).
- [19] H. Geissel, GSI Report 97-03 (1997).
- [20] H. Simon *et al.*, to be published.